

EFFECTS OF CHAMBER GEOMETRY AND GAS PROPERTIES ON HYDRODYNAMIC EVOLUTION OF IFE CHAMBERS

Zoran Dragojlovic¹ and Farrokh Najmabadi²

*Department of Electrical & Computer Engineering and Center for Energy Research,
University of California in San Diego, 9500 Gilman Drive, La Jolla, CA 92093-0417*

¹zoran@fusion.ucsd.edu, ²najmabadi@fusion.ucsd.edu

The rep rate of an inertial fusion energy facility depends on the time-dependent response of the chamber environment between target ignitions. The fusion burn following the target ignition releases large quantities of energy into the chamber. This energy should be removed and the environment should be returned to a quiescent state so that the new fusion target can be positioned for the next cycle. Understanding the hydrodynamic transport of this energy through the chamber fill gas is essential because the multidimensional geometry effects become important on the long time scale, as the fluid interacts with the vessel wall containing various beam access ports. This interaction affects several different modes of the chamber species transport, including convection induced by shock waves and secondary flow, molecular diffusion, electron conductivity and radiation. In order to investigate these phenomena, we have developed SPARTAN code as an assembly of algorithms that were the most suitable for an accurate treatment of the computational problem, such as shock wave resolution and tracking, underlying flow physics and complex wall geometry. This study demonstrates that the geometry effects are critical in affecting the flow during the first 50 milliseconds following the target ignition. Thermal diffusion by molecules and free electrons has only a moderate effect in reducing the temperature extrema and is not sufficient to cool down the chamber to the equilibrium with the chamber wall within 100 ms. Radiation of the background plasma was identified as the only transport mechanism that has approached to this goal, making the chamber environment more suitable for inserting the next target.

I. INTRODUCTION

The evolution of an inertial fusion energy (IFE) chamber following the target ignition and the underlying transport phenomena can be separated into two phases based on the vast difference in the relevant time scales. The target ignition lasts for less than a nanosecond and is followed by the release of X-rays (mostly from bremsstrahlung radiation), neutrons (fusion products) and

ions (fusion products and target debris). The X-rays and ions travel through the chamber and deposit some of their energy in the chamber background gas. The absorbed energy is immediately released through radiation, resulting in the gas temperature decay to a few eV's. After this initial fast process, the chamber evolves in a hydrodynamic time scale. This "hydrodynamics" phase is characterized by further redistribution of the energy through the chamber by convection, conduction, and radiation.. This second phase lasts for 100-200 ms, until the ignition of the next target. A summary description of various physical phenomena occurring in an IFE chamber can be found in Ref. [1]

Our research effort is directed towards development of a fully integrated computer code which has a capability to model and study the chamber dynamic behavior in the "long" time scale, including: the hydrodynamics; the effects of various heat sources and transfer mechanisms such as photon and ion heat deposition and chamber gas conduction, convection and radiation; the chamber wall response and lifetime; and the cavity clearing. TSUNAMI code was developed in order to understand the gas dynamics of liquid protected reactors, such as HYLIFE, Ref. [2]. The time scale of interest for these simulations is of the order of microseconds, where the effects of diffusion and radiation heat transfer can be neglected. Besides, TSUNAMI solver is based on a single upwind scheme that might not be sufficiently accurate for the long time scale and strong discontinuities of the IFE chamber.

We have developed SPARTAN code as an assembly of state-of-the-art algorithms suitable for an accurate treatment of the IFE chamber dynamics and evolution, including shock wave resolution and tracking, underlying flow physics, and complex wall geometry. At present, SPARTAN solves 2-D transient compressible Navier-Stokes equations with Cartesian and cylindrical geometry. The code is written in a modular fashion so that extrapolation to 3-D geometry is straightforward. Behavior of strong shocks born out of the target blast is captured accurately by a second order Godunov algorithm. Diffusive terms (viscosity and thermal conductivity) and volumetric sources are included and can

depend on multiple local state variables, such as density and temperature. Uniform accuracy throughout the fluid domain is obtained by adaptive mesh refinement. This is essential as the width of the shock region is usually several orders of magnitude smaller than the chamber dimensions. Arbitrary chamber geometry is incorporated into a Cartesian grid and resolved by embedded boundary method.

A short summary of numerical algorithms incorporated into SPARTAN is given in Section II. For a more detailed analysis, the reader is referred to [3]. In Section III we present simulations to analyze the impact of chamber geometry, molecular diffusivity and background plasma on the chamber state evolution. Conclusions and future plans with SPARTAN are given in Section IV.

II. NUMERICAL METHOD

The computational approach used in this study consists of an assembly of several algorithms that are the most appropriate for the problem at hand and well documented in the literature. The base numerical scheme is a second order Godunov method on the Cartesian grid, used for solving compressible Euler equations, as referenced in [4]. The intersection between the Cartesian grid and the fluid domain boundary is interpreted by irregular cells. In the cells away from the boundary, the solution is advanced by an explicit, second order advection scheme. The fluxes into the partial cells are treated in a special post-processing step which guarantees the uniform accuracy, consistency and stability throughout the entire computational domain. The accuracy of the base scheme in the irregular cells was improved by interpolation of fluxes onto the centroids of the cell faces, as outlined in Ref. [5]. In addition, the diffusive terms such as viscosity and conduction, as well as volumetric source terms such as radiation were added by utilizing the ideas which first appeared in [6] and were applied to solving the Poisson's equation by the Cartesian grid method. An iterative Runge-Kutta update of diffusive and volumetric terms was used in order to account for the temporal dependence of fluid properties. The resulting assembly of algorithms was incorporated into a block-structure adaptive mesh refinement method, documented in [4, 7]. SPARTAN's adaptive mesh refinement algorithm organizes the computational grids into levels which vary in grid density from coarse to fine. The fluid domain is defined on the coarsest level grid. A tagging algorithm runs on this level at every time step and marks all the cells that have a high difference in density or energy across them. Higher-level grids are placed over the tagged cells, then the tagging algorithm runs again until either the highest grid level is reached or the refinement criteria are satisfied. The grid is refined at every time step as the solution rapidly changes. Detailed convergence analyses and a sample application relevant to IFE chamber scenarios are used to validate the

assembled algorithm in a simplified two-dimensional, non-adaptive setting, as shown in Ref. [3]. The method includes 2-D Cartesian and cylindrical geometry and is extensible to 3-D.

III. SIMULATION MODELS

In order to provide a multi-dimensional view of the chamber gas dynamics, the flow and heat transfer mechanisms were simulated in two mutually orthogonal planes. The chamber is shaped as a cylinder, is shown in Figure 1. The Cartesian model depicted in Figure 1. (a) was used for simulating the flow in the plane parallel to the chamber base (x-y), assuming that everything along the chamber axis is constant. The cylindrical model shown in Figure 1b was used for observing the perpendicular, r-z plane, assuming a complete symmetry in the polar angle θ . The chamber diameter is 13 m and equals the chamber height. In the Cartesian model, the arrays of laser beam lines along the z axis were substituted by four beam sheets I-IV. In the cylindrical model, the array of beam lines around the perimeter of the chamber is substituted by a single disk shaped beam sheet denoted by V. In addition, two tube shaped beam lines VI and VII are added on top and bottom of the chamber, respectively. All the beam lines are 20 m long and 1 m wide. Prior to the target ignition, the chamber was filled with Xe gas at a pressure of 6.67 Pa (50 mTorr) and room temperature. The direct drive target [8] has a yield of 160 MJ. The target explosion is modeled by the 1-D Lagrangian code BUCKY [9]. The target X-rays and ions heat the Xe gas, which is subsequently cooled through radiation. The chamber state at 500 μ s was estimated by BUCKY. At this point in time, the Xe gas in the chamber has cooled down to about 2 eV and radiation losses have become negligible. At the same time, the shock wave from target explosion has not yet reached the chamber wall, and therefore, 1-D results from BUCKY can be interpolated for analysis with a higher-dimension code such as SPARTAN.

BUCKY's results [10] have been used as the initial condition for SPARTAN. The initial conditions were interpolated onto the 2-D grid by rotating the 1-D BUCKY solution about the blast location, as is shown in Figure 1. The same interpolation makes the initial shock wave cylindrical in the Cartesian representation of the problem and spherical in the cylindrical representation of the problem. For simulations reported here, SPARTAN is exercised with a single species, i.e. chamber Xe gas. The chamber gas is represented by an ideal equation of state. The viscosity and thermal conductivity of neutral gas are dependent on temperature, as specified by the semi-empirical expression:

$$\eta(T) = \eta_o \left(\frac{T}{T_{o,\eta}} \right)^{1.5} \frac{T_{o,\eta} + T_{s,\eta}}{T + T_{s,\eta}} \quad (1)$$

where viscosity μ and conductivity k should be substituted for the general property η . The conductivity-related constants in this model $T_{s,k}$, $T_{o,k}$ and k_o were determined by fitting the experimental data reported in ref. [11] on the interval (800, 2,000)K. The equivalent constants for viscosity, $T_{s,m}$, $T_{o,m}$ and μ_o were based on the experimental data found in Ref. [12].

Simulations of neutral gas with SPARTAN, Ref. [13], indicated that the temperature in the chamber quickly rises from the initial 2 eV to 40 eV, due to convergence of the reflected shock into the chamber center. As a result, there exists a background plasma in the chamber. The plasma affects the chamber state by electron heat conduction and radiation. We assume a coronal equilibrium in the chamber gas, which uniquely determines the electron density, ion density and the radiated power per unit volume as functions of density and temperature of the gas [14]. The thermal conductivity of the mixture was obtained by adding up the contributions from neutral molecules and the electrons. The radiation was modeled as a volumetric heat sink incorporated in the Navier-Stokes equations.

The boundary conditions on the wall include zero mass flux and reflective momenta with wall shear stress based on no-slip condition. The energy flux is determined by heat conduction from the fluid to the wall. The wall temperature was set at 700°C.

IV. RESULTS AND DISCUSSION

Figure 2 shows “snapshots” of the temperature distribution in the IFE chamber filled with neutral gas, at different times after the target ignition.

Within the first 3 milliseconds of the target ignition, a shock wave produced by the rapid heating of the background gas by x-ray and ions from the target ignition travels through the chamber, reflecting from the wall and converging back into the center of the chamber. The resulting compression generates a hot central core of the chamber which spans about 50% of the chamber radius and reaches the temperatures of around 40-55 eV. The lower value of temperature was predicted by the Cartesian model, while the cylindrical model exhibited the stronger compression, which can be explained by the influence of the shock geometry relative to the chamber.

During the next 10-20 milliseconds, the pressure wave remains relatively coherent and oscillates three more times through the chamber. This stirs up the fill gas without causing any further compressive heating. As a

result, the hot chamber core spreads out towards the wall and drops in temperature by 50%.

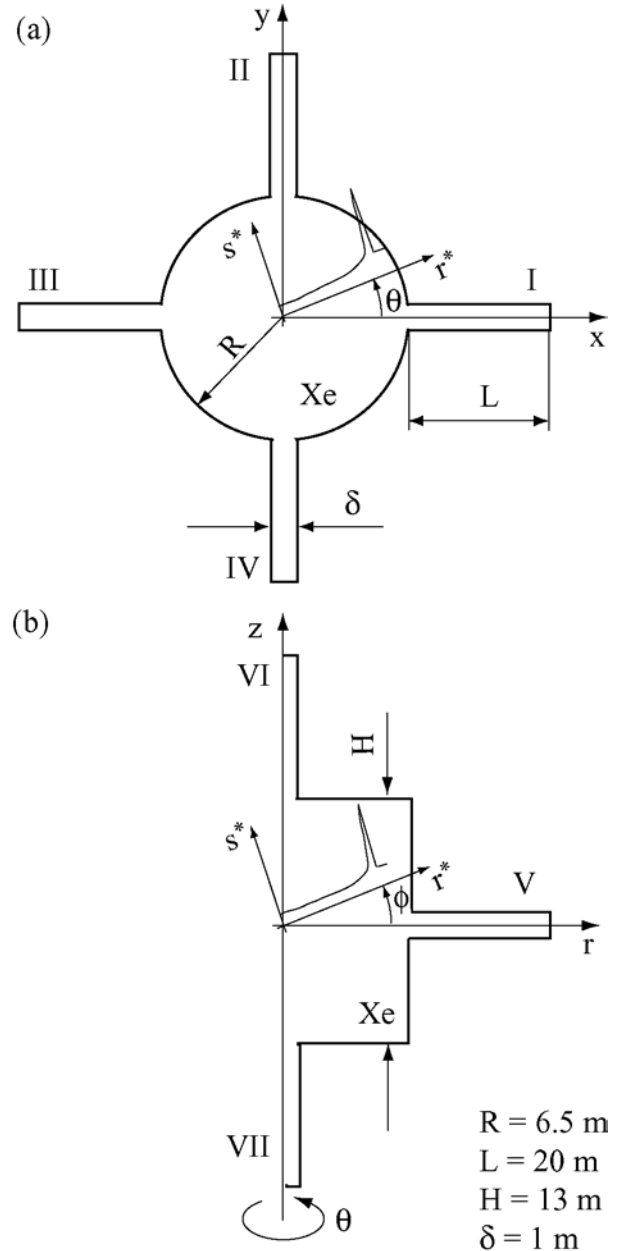


Figure 1. Geometry and initial conditions for the IFE chamber. Wall configuration for the Cartesian model is given in (a), while the corresponding cylindrical model is depicted in (b). Chamber body is a cylinder of a radius R and a height H , with size values provided in the figure. The final optics elements are denoted by Roman Numerals I-VII. All the beam elements have the same length L and width δ . The 1-D solution from BUCKY is sketched with a diagram $S^*(r^*)$.

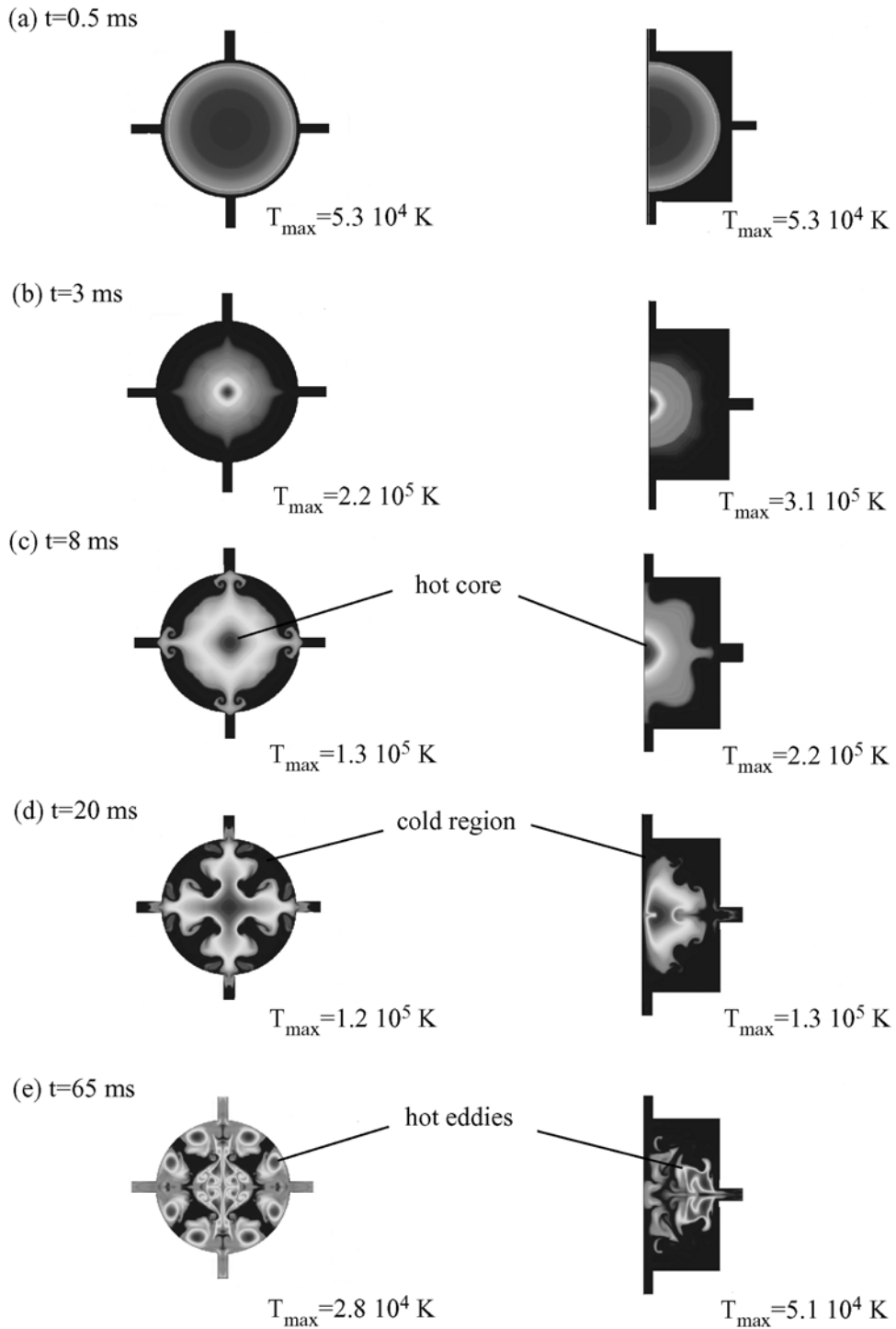


Figure 2. Temperature distribution in the IFE chamber filled with neutral gas at several characteristic times. Results of the Cartesian model are given on the left while simulations with cylindrical geometry are shown on the right. Cases (a-d) feature a hot central region, surrounded by the cold gas. In case (e), the high temperature core has transformed into hot eddies, which have relocated close to the walls.

Between 13 milliseconds and 65 milliseconds from the target blast, a secondary flow develops as a result of the interaction between the initial shock and the beam line structure of the chamber. This flow has a crucial role in the chamber evolution due to:

1. Breaking apart the hot core of the chamber into several smaller regions by radially non-uniform stirring.
2. Reducing the peak temperatures in those regions by an order of magnitude compared to the initial core.
3. Bringing the hot “eddies” closer to the chamber wall where they can further cool down by heat conduction.

From 65 milliseconds to 100 milliseconds past the target ignition, the flow geometry remains the same.

It should be noted that the Cartesian and cylindrical models predict the same trend in flow. In fact, they may be interpreted as views of a 3-D chamber from two different angles. For example, the Cartesian interpretation of the temperature field at 65 ms gives a top view, showing the array of hot eddies which formed as a result of beam channel distribution in the x-y plain but it does not reveal how the eddies distribute in the vertical plain, with respect to the channels. The cylindrical version depicted on the right gives a side view of the chamber, demonstrating that the eddies will tend to distribute above and below the channel entrance and not in front of the channel.

To examine the main modes of energy transport in the chamber, we considered three different test cases:

Case I: Energy transport through conduction by the neutral gas only;

Case II: Energy transport through conduction by neutral gas and free electrons of the background plasma and

Case III: Energy transport through conduction by neutral gas and free electrons of the background plasma and radiation.

The impact of heat conduction and radiation on the total internal energy of the chamber system is shown in Figure 3.

Figure 3a shows that during the first 20 ms, the internal energy of chamber gas does not change after the initial compressive heating. During this time, the conductive heat loss into the wall does not occur because the hot gas is located at the core of the chamber and away from the wall. During this period, several weak compressions occur, as denoted by the local peaks of internal energy and the kinetic energy.

Around 20 milliseconds past the target ignition the hot gas that has been diffusing from the core of the chamber touches the wall and the uniform conduction to the wall

becomes the only mode of cooling the chamber until the next shot of the target.

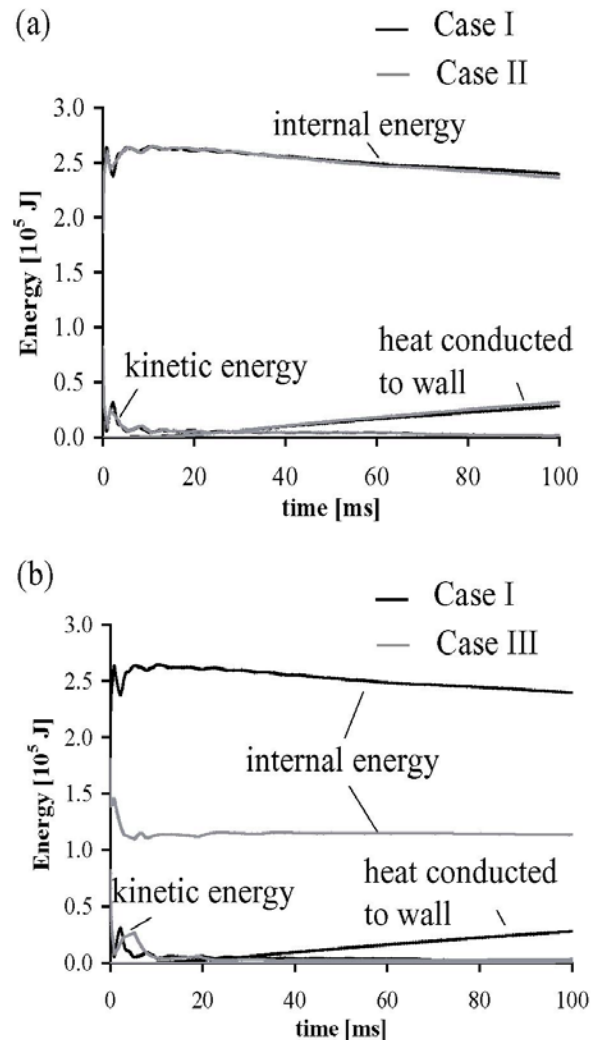


Figure 3. Temporal evolution of gas energy. Case I represents neutral gas. Case II represents neutral gas with conductivity of free electrons in addition to molecular conductivity. Case III includes molecular conductivity, conductivity of free electrons and radiation due to background plasma.

It is clear from this figure that a) The effects of electron thermal conductivity is negligible, and b) In both cases, the internal energy of the system was reduced only by 5% - conduction is not very effective in cooling the chamber. Figure 3b, however, shows that the radiation from the background plasma (Case III) has a tremendous effect on the internal energy of the chamber. Heat generated by the initial compression of the shockwave is almost instantly radiated from the chamber cavity into the surrounding environment. During the first 10 milliseconds, the internal energy drops to about 110 kJ from its initial value, which corresponds to an average gas temperature of 2000K. At this temperature radiation diminishes and the gas further cools down via conduction.

Figure 4 compares the temperature fields in the chamber for the three cases of heat transfer. Both Cartesian and cylindrical geometry models are shown. Figure 4 shows that the electron conductivity helps in acquiring a more even temperature distribution across the Cartesian chamber volume and in the mid-section of the axially-symmetric chamber. This results in lowering the temperature peaks in both Cartesian and cylindrical chamber. Adding radiation to the model changes the flow regime by substantially cooling down the gas compared to the previous two cases and reducing the effects of molecular and electron diffusivity on the flow. As a result, a larger number of small eddies is set up and the chamber state is more quiescent overall.

IV. CONCLUSIONS

Overall, SPARTAN simulations of the hydrodynamic evolution of an IFE chamber indicate:

1. Three-dimensional effects of chamber geometry are critical in assessing the chamber dynamics.
2. Radiation of background plasma is the most important mechanism for heat transfer.
3. Molecular diffusivity and diffusivity of free electrons have only a moderate impact on cooling down the chamber system and damping out the flow.

The dynamics and evolution of the chamber appears to be rather complex. The interactions between the shock waves and the beam structure of the chamber generates a secondary flow which has a crucial role in stirring up the chamber and redistributing the heat generated by the target explosion and the initial compression. The compressive and viscous heating of the gas diminishes within the first 40 milliseconds from the target blast. After that, the chamber cools rather uniformly. The cooling rate by thermal conduction is insufficient to bring the fill gas to the equilibrium with the chamber wall.

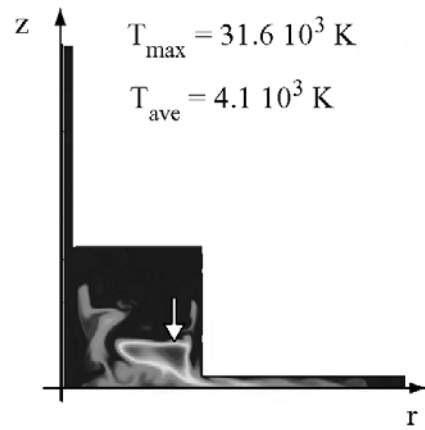
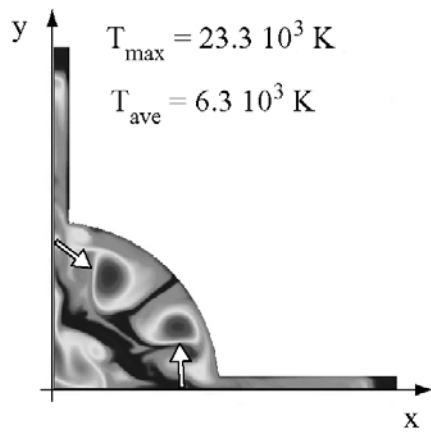
The background plasma stemming from the hot central core region of the chamber affects the chamber evolution by the means of electron conductivity and radiation.

Compared to the neutral gas, the electron conductivity lowers the temperature peaks in the chamber by a factor of two but it does not significantly improve the cooling rate of the chamber as a system. This can be explained by the fact that the chamber cools down only by the conduction to the wall. The cold near-wall region is predominantly neutral and acts as a baffle to electron conduction. The cooling of the chamber by radiation has a tremendous impact on the final chamber state. As a result, the chamber gas temperature is much lower and the chamber state is considerably more quiescent than in the simulations that ignore the background plasma.

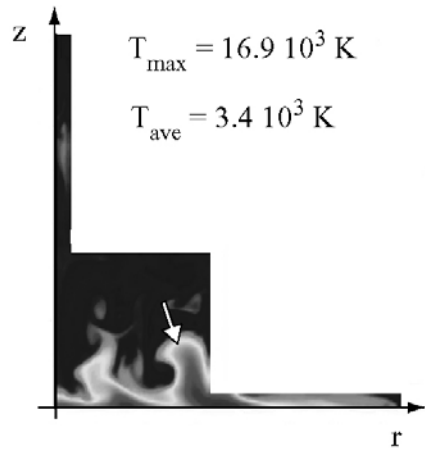
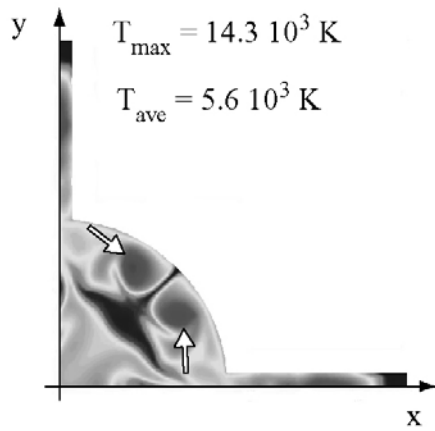
It should be emphasized that none of the three modes of cooling (conduction, convection, and radiation) are sufficient to bring the gas temperature in equilibrium with the wall temperature in 100 ms. In reality, after several shots, a quasi-equilibrium will be achieved in the chamber where the initial and final energy state of the chamber are identical. This quasi-equilibrium can be, in principle, found by iterative simulations with BUCKY and SPARTAN and is planned.

We have explored the 3-D geometrical effects by 2-D simulations of flow in two mutually perpendicular planes: one parallel to the chamber base and one encompassing the axis of the chamber. We find many similarities between the two flow models, even though the former approximates the initial shock wave as a cylinder while the latter correctly represents it as a sphere. Both models predict generation of the hot, one-dimensional core of the chamber which evolves into eddy-like hot regions that tend to distribute between the channels and close to the wall. For the given geometry, the resulting flow configuration consists of two layers of concentric arrays of eddies placed one above the other. By adding more beam channels, we can contemplate that we would have obtained multiple layers of numerous small eddies lying on top of each other and evenly distributed between the channels. This is supported by our earlier Cartesian models of the IFE chamber, which indicated that adding the channels around the perimeter of the chamber resulted in obtaining a larger number of smaller eddies and better stirring of the hot gas. Even though all the important flow trends are identified in this study, further exploration with a 3D numerical model can provide a more detailed picture.

Case I



Case II



Case III

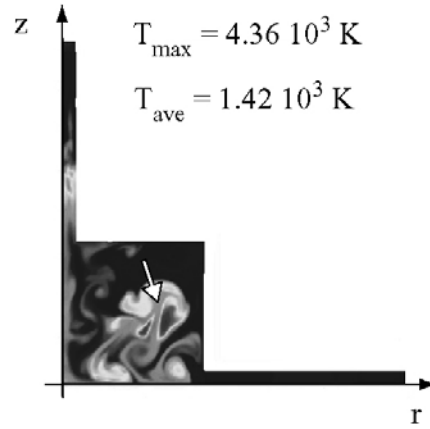
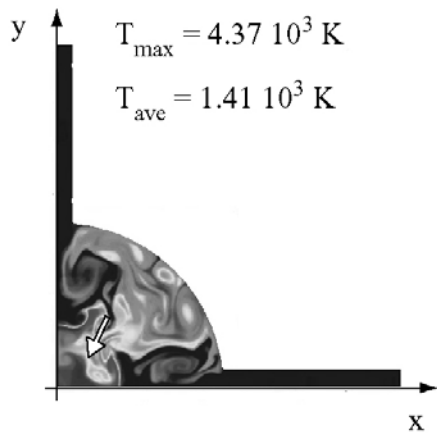


Figure 4. Chamber temperature at 100 milliseconds, for three different cases of heat transfer and for two different geometries. The Cartesian models are shown in the left column, while cylindrical models are placed in the right column. The hottest regions in the chamber are marked by arrows.

ACKNOWLEDGMENTS

This research was supported by the Naval Research Laboratory under grant N00173-02-1-6010.

REFERENCES

- [1] G. A. MOSES, R. R. PETERSON: "Computer Modeling of ICF Target Chamber Phenomena", *Laser and Particle Beams* (1994), volume 12, no. 2, pp. 125-162.
- [2] X. M. CHEN, V. E. SCHROCK, P. F. PETERSON, "Gas Dynamics in the Central Cavity of the HYLIFE-II Reactors," *Fusion Technology* **21** (1992).
- [3] Z. DRAGOJLOVIC, F. NAJMABADI, M. DAY: "An Embedded Boundary Method for Viscous, Conducting Compressible Flow", *Journal of Computational Physics*, submitted for publication.
- [4] R. B. PEMBER, J. B. BELL, P. COLELLA, W. Y. CRUTCHFIELD, M. L. WELCOME, "An Adaptive Cartesian Grid Method for Unsteady Compressible Flow in Irregular Regions", *Journal of Computational Physics*, 120:2, pp. 278-304, Sept. 1995.
- [5] D. MODIANO, P. COLELLA: "A Higher-Order Embedded Boundary Method for Time-Dependent Simulation of Hyperbolic Conservation Laws", *Proceedings of FEDSM'00*, 2000.
- [6] JOHANSEN, P. Colella: "A Cartesian Grid Embedded Boundary Method for Poissons Equation on Irregular Domains", *Journal of Computational Physics*, Volume 147(1), pp. 60-85, 1998.
- [7] A. S. ALMGREN, J. B. BELL, P. COLELLA, ET. AL, *Journal of Computational Physics*, Volume 142, pp. 1-46, 1998.
- [8] S. E. BODNER, D. G. COLOMBANT, A. J. SCHMITTAND M. KLAPISCH, *Physics of Plasmas*, Volume 7, pp. 2298-2301, 2000.
- [9] J. J. MACFARLANE, G. A. MOSES, R. R. PETERSON, University of Wisconsin, Fusion Technology Institute Report UWFD-984, 1995.
- [10] D. HAYNES, Los Alamos National Laboratory, private communications.
- [11] JAIN, P. C.: "The Prediction of the Thermal Conductivity of Xenon", *Journal of Physics, Division: Applied Physics*, Volume 11, pp. 2371-2372., 1978.
- [12] MCCARTY, R. D.: "Correlations for the Thermophysical Properties of Xenon", National Institute of Standards and Technology, Boulder, CO, 1989, 00.
- [13] Z. DRAGOJLOVIC, F. NAJMABADI: "Simulation of IFE Chamber Dynamic Response by a Second Order Godunov Method with Arbitrary Geometry", *Inertial Fusion Sciences and Applications* (2003), pp. 850-853.
- [14] G. A. MOSES, University of Wisconsin, Madison, private communications.